Neuropharmacology xxx (2014) 1–15

Contents lists available at ScienceDirect

Neuropharmacology

journal homepage: www.elsevier.com/locate/neuropharm

Kinetic properties and open probability of α7 nicotinic acetylcholine receptors

Krisztina Pesti [a,b], Anett K. Szabo [a,b], Arpad Mike [b,*], E. Sylvester Vizi [b]

[a] Semmelweis University, School of Ph.D. Studies, Üllői út 26, H-1085 Budapest, Hungary
[b] Laboratory of Molecular Pharmacology, Institute of Experimental Medicine, Hungarian Academy of Sciences, P.O.B. 67, H-1450 Budapest, Hungary

ARTICLE INFO

Article history:
Received 23 March 2013
Received in revised form
13 January 2014
Accepted 21 January 2014

Keywords:
α7 nicotinic acetylcholine receptor
Choline
PNU-120596
Kinetic modeling

ABSTRACT

Alpha7 nicotinic acetylcholine receptor (nAChR) has some peculiar kinetic properties. From the literature of α7 nAChR-mediated currents we concluded that experimentally measured kinetic properties reflected properties of the solution exchange system, rather than genuine kinetic properties of the receptors. We also concluded that all experimentally measured EC_{50} values for agonists must inherently be inaccurate. The aim of this study was to assess the undistorted kinetic properties of α7 nAChRs, and to construct an improved kinetic model, which can also serve as a basis of modeling the effect of the positive allosteric modulator PNU-120596, as it is described in the accompanying paper. Agonist-evoked currents were recorded from GH4C1 cells stably transfected with pCEP4/rat α7 nAChR using patch-clamp and fast solution exchange. We used two approaches to circumvent the problem of insufficient solution exchange rate: extrapolation and kinetic modeling. First, using different solution exchange rates we recorded evoked currents, and extrapolated their amplitude and kinetics to instantaneous solution exchange. Second, we constructed a kinetic model that reproduced concentration-dependence and solution exchange rate-dependence of receptors, and then we simulated receptor behavior at experimentally unattainably fast solution exchange. We also determined open probabilities during choline-evoked unmodulated and modulated currents using nonstationary fluctuation analysis. The peak open probability of 10 mM choline-evoked currents was 0.033 ± 0.006, while in the presence of choline (10 mM) and PNU-120596 (10 μM), it was increased to 0.599 ± 0.058. Our kinetic model could adequately reproduce low open probability, fast kinetics, fast recovery and solution exchange rate-dependent kinetics.

1. Introduction

The α7 subunit containing nicotinic acetylcholine receptor (α7 nAChR) is known as the second most abundant nicotinic receptor type in the CNS (after the α4β2 type receptor). These receptors mostly but not exclusively are homopentamers of the α7 subunit. Their most prominent role within the central nervous system is probably the pre- and postsynaptic modulation of synaptic function and plasticity (Albuquerque et al., 2009; Alkondon and Albuquerque, 2001; Gray et al., 1996; Gu and Yakel, 2011; Lendvai and Vizi, 2008; Lozada et al., 2012; Rozsa et al., 2008; Vizi and Lendvai, 1999), which is the basis of their role in cognition (Hurst et al., 2012; Lendvai et al., 2012; McKay et al., 2007).

The α7 nAChR has some unique properties: a high Ca^{2+} permeability, which is counterbalanced by extremely fast desensitization, causing a fast onset and decay kinetics and an extremely low open probability (Williams et al., 2012, 2011).

The aim of this study was to refine the kinetic analysis of the receptor. In order to clearly see the unusual aspects of α7 nAChR receptor kinetics, we need to briefly review what is known about the kinetic properties of this receptor (Section 3.1.). This re-examination of reported properties, makes it evident that the kinetics depends both on agonist concentration and on solution exchange rate. The nature of these dependences, and their interaction will be discussed, together with their possible mechanism. From the apparent solution exchange rate dependence it follows that measurements of the intrinsic kinetic properties of the receptor may be problematic, and experimentally measured kinetics may misrepresent intrinsic kinetics of the receptor.

One of our aims was to give a more accurate estimation of intrinsic kinetic properties of α7 nAChRs, i.e., receptor kinetics undistorted by insufficient solution exchange rate.

Abbreviations: α7 nAChR, α7 subtype nicotinic acetylcholine receptor; PNU-120596, 1-(5-chloro-2,4-dimethoxyphenyl)-3-(5-methylisoxazol-3-yl)urea; SXT, 10–90% solution exchange time.

* Corresponding author. Tel.: +36 12109971; fax: +36 12109423.
E-mail address: mike@koki.hu (A. Mike).

0028-3908/$ – see front matter © 2014 Elsevier Ltd. All rights reserved.
http://dx.doi.org/10.1016/j.neuropharm.2014.01.034

Our second major goal was to propose a plausible kinetic scheme for major conformational states of the receptor. This is important if we want to understand the mechanism of receptor gating behavior: its agonist concentration-dependence, its solution exchange rate-dependence, and the interaction of the two. As we will describe in Section 3.3.1., none of the kinetic models thus far constructed by our group or others could sufficiently reproduce experimental behavior. Furthermore, an acceptable kinetic model allows the estimation of intrinsic properties, *i.e.*, determination of approximate rate constants of agonist association/dissociation, receptor opening, closing and desensitization.

Constructing an acceptable kinetic model was important for another reason: One of our aims was to study the mode of action of the positive allosteric modulator PNU-120596.

The mode of action of a modulator can be quantitatively described if when we can explain *which* exact conformational transitions are modified, and *how much* they are modified. Does the modulator affect agonist association, agonist dissociation, activation, deactivation, desensitization or recovery? In terms of Markov models: which specific rate constants are increased or decreased in modulator-bound states, and by what factor? Results of this study are presented in the accompanying paper {Szabo, #171}.

Finally, the low open probability during agonist evoked currents are one of the unique properties of α7 nAChRs, and it is essential that the kinetic model we construct can reproduce this attribute also. We therefore aimed to determine peak open probability values during agonist evoked receptor activation. The number of open receptors could be deduced from amplitude-variance plots of agonist-evoked currents, but in the case of the α7 nAChRs the mean open time is so low, that a significant part of the variance is lost due to unresolvable fast openings. Because the positive allosteric modulator PNU-120596 has been shown to radically prolong channel open times, and thereby to induce prolonged tail currents in the absence of the agonist (daCosta et al., 2011; Williams et al., 2011), we were able to construct amplitude-variance plots undistorted by channel block, or by unresolvably fast openings and determine open probability values. Details of the mechanism of action for PNU-120596 are described in the accompanying paper {Szabo, #171}.

2. Materials and methods

2.1. Materials

Methyllycaconitine and PNU-120596 were obtained from Tocris Bioscience (Bristol, UK). Cell culture products were obtained from Life Technologies™. All other chemicals were obtained from Sigma.

2.2. Cell culture

GH4C1 cells stably transfected with pCEP4/rat α7 nAChR were obtained from Siena Biotech S.p.A. (Siena, Italy). Cells were cultured in poly-L-lysine coated Petri dishes using HAM's F10 medium supplemented with 15% horse serum, 2.5% fetal bovine serum, 1% penicillin–streptomycin, 1 mM GlutaMAX, 100 μg/ml Hygromycin B.

2.3. Electrophysiology

Experiments were performed in whole-cell or outside-out patch configurations, using an Axopatch 200B amplifier and the pClamp software (Molecular Devices, Sunnyvale, CA). Currents were recorded at −70 mV; digitized at 100 kHz (in short protocols where currents were evoked by choline alone) or at 20 kHz (in longer protocols where the effects of PNU-120596 were studied) and filtered at 10 kHz. For illustration and data analysis some of the traces were further digitally filtered off-line at 2 kHz. Borosilicate glass pipettes (1.3–4.8 MΩ) were filled with pipette solution of the following composition (in mM): CsCl 55, CsF 65, EGTA 10, HEPES 10 (pH = 7.2). The extracellular solution contained the following (in mM): NaCl 140, KCl 5 $CaCl_2$ 2, $MgCl_2$ 1, Glucose 5, and HEPES 5, (pH = 7.3). Solution exchange was performed by the "liquid filament switch" method (Franke et al., 1987; Jonas, 1995) using 1.5 mm OD theta glass tubes (Harvard Apparatus, Holliston, MA) and a Burleigh LSS-3200 ultrafast solution switching system. Theta tubes were pulled and broken to have a tip diameter between 150 and 250 μm. A drop of Sylgard® was injected close to the tip of both theta glass channels, half-cured, penetrated by a 0.35 mm OD Microfil™ capillary (WPI Inc., Sarasota FL), and cured fully. Tubing was connected to the inlets of Microfil™ micropipettes. The solution reservoirs were connected to the pressure control unit of a DAD-12 solution exchange system (ALA Scientific Instruments Inc., Farmingdale, NY), this allowed optimization of flow rate (typically ~0.2–0.3 ml/min, which corresponded to 5–20 cm/s flow velocity), and fast exchange of solutions (flow rate increased up to ~1 ml/min). The total dead volume of the tubing from the reservoir to the tip of the theta tube was ~150 μl. Voltage command waveforms for the piezoelectric actuator were written in the pClamp software, and delivered through an analog output of the Digidata 1322A interface. In a few experiments the pressure-controlled dual U-tube system (Szasz et al., 2007) was used for solution exchange, pressure-control was provided by the same DAD-12 instrument. In addition to the fast drug application systems, a permanent laminar flow of extracellular solution at a rate of ~2.5 ml/min was present in the recording chamber throughout the experiments. The osmolarity values of the control extracellular solution, as well as the 10 mM ACh and 10 mM choline solutions were set to 320 mOsm, and all other agonist concentrations were made as a mixture of these.

2.4. Simulations

The simulation was based on a set of differential equations with the occupancy of each receptor state (i.e., the fraction of the receptor population in that specific state) given by the following equation

$$\frac{dS_i(t)}{dt} = \sum_j^n (S_j(t)*k_{ji} - S_i(t)*k_{ij})$$

where $S_i(t)$ is the occupancy of a specific state at the time t, $S_j(t)$ is the occupancy of a neighboring state, n is the number of neighboring states, and k_{ij} and k_{ji} are the rate constants of transitions between neighboring states. All simulations were performed using Berkeley Madonna v8.0.1 (http://www.berkeleymadonna.com/), to solve the differential equations using a fourth-order Runge–Kutta method. All parameters were adjusted manually.

2.5. Analysis of data

Curve fitting was performed by the Solver function of Microsoft Excel. The Bateman function: $I(t) = k_1/(k_1-k_2) * \exp(-k_2 * t) - \exp(-k_1 * t)$ was used to fit choline-evoked currents and to obtain apparent rate constants of activation and desensitization. Decay phases of evoked currents were fit with either monoexponential or biexponential functions: $I(t) = (I_{max}-I_{min}) * \exp(-t/\tau) + I_{min}$ and $I(t) = (I_{max}-I_{min}) * [A_1 * \exp(-t/\tau_1) + A_2 * \exp(-t/\tau_2)] + I_{min}$, where τ_1 and τ_2 are the time constants, and A_1 and A_2 are their respective contribution to the amplitude. Exchange rate dependence plots were fit with linear ($y = a*t + b$), monoexponential ($y = a*\exp(t*\tau) + b$) biexponential ($y = a_1*\exp(t*\tau_1) + a_2*\exp(t*\tau_2)$) or power ($y = a*(x+b)t$) functions; where a, a_1, a_2, b, τ, τ_1 and τ_2 are constants, and t is the 10–90% solution exchange time (SXT). Paired Student's t test was used for statistical analysis. A probability level of 0.05 or less was considered to reflect a statistically significant difference.

3. Results and discussion

3.1. Background: concentration-dependent and solution exchange rate-dependent kinetics of α7 nAChR-mediated currents

Rat α7 nAChR expressing GH4C1 cells were used at 2–5 days after passage. Agonist application was performed by a pressure-controlled theta tube perfusion system. Whole cells or outside-out patches were lifted to the mouth of the theta-tube.

3.1.1. Concentration-dependent kinetics

The effect of different concentrations of ACh and choline was investigated. As it has been previously observed we found that with increasing agonist concentration: i) the onset kinetics is accelerated, ii) the decay kinetics is accelerated, and iii) the current amplitude is increased. Examples for the concentration-dependent kinetics has been shown in several papers, but typically has not been quantified. For this reason, we have reviewed these figures, measured rise times, and estimated decay time constants (exponential curves were overlaid with the figures after adjusting axes to the calibration bars, and time constants were adjusted until the fit seemed visually acceptable). The results from 9 individual publications (Alkondon and Albuquerque, 1993; Castro and

Please cite this article in press as: Pesti, K., et al., Kinetic properties and open probability of α7 nicotinic acetylcholine receptors, Neuropharmacology (2014), http://dx.doi.org/10.1016/j.neuropharm.2014.01.034

Albuquerque, 1993; Friis et al., 2009; Gopalakrishnan et al., 1995; Mike et al., 2000; Papke, 2006; Papke and Thinschmidt, 1998; Puchacz et al., 1994; Williams et al., 2012) together with our current data are plotted in Fig. 1. The concentration-dependent change in onset and decay kinetics is obvious. The relationship between log(rise time) and log[ACh] was close to linear, while the slope of the log(decay time constant) vs. log[ACh] plot decreased at high concentrations. While these observations were true for all studies, it was strange to see, that time-to-peak values and decay time constants varied between individual studies by more than three orders of magnitude. We wondered what the reason might be for recording currents with such diverse kinetics.

3.1.2. Solution exchange rate-dependent kinetics

In our experiments we observed that solution exchange rate has a very similar effect on α7 nAChR mediated currents: As the solution exchange rate was increased: i) the onset kinetics was accelerated, ii) the decay kinetics was accelerated, and iii) the amplitude was increased (see Section 3.2.2.). Could this phenomenon account for such great differences? We are aware of only one publication where the effect of solution exchange rate on α7 nAChR-mediated currents was studied (Fedorov et al., 2012), and in this case it was only investigated within a narrow range (fourfold change in solution exchange times). In the literature, however, solution exchange rates differ by several orders of magnitude. We reviewed publications where the solution exchange rate was indicated (Alkondon and Albuquerque, 1993; Bouzat et al., 2008; Castro and Albuquerque, 1993; Friis et al., 2009; Gopalakrishnan et al., 1995; Mike et al., 2000; Papke et al., 2000; Papke and Thinschmidt, 1998). Measured rise time and decay time constants for 1 mM ACh-evoked currents from these papers, as well as from this current study (see Section 3.2.2.) were plotted against solution exchange rates. The results (Fig. 2) show an unmistakable correlation between the measured kinetics of currents and solution exchange rates.

We believe that the two phenomena are caused by the same remarkable property of the receptor. As it has been demonstrated first by Papke and Thinschmidt (1998), current amplitude and kinetics do not seem to be determined by agonist concentration itself, but rather by the concentration *gradient*: the rate of concentration increase at the onset phase of agonist application. As it has been shown, the onset and decay kinetics of the current is so fast, that the peak amplitude occurs already during the early onset phase of the agonist pulse, well before the solution exchange is complete, *i.e.*, when the nominal agonist concentration to be perfused has not yet been reached. The response we measure is not to the nominal concentration, but to a lower concentration (Papke et al., 2000; Papke and Thinschmidt, 1998; Uteshev et al., 2002). If we consider the case when two agonist pulses are given with equal concentration gradient but different final nominal concentration,

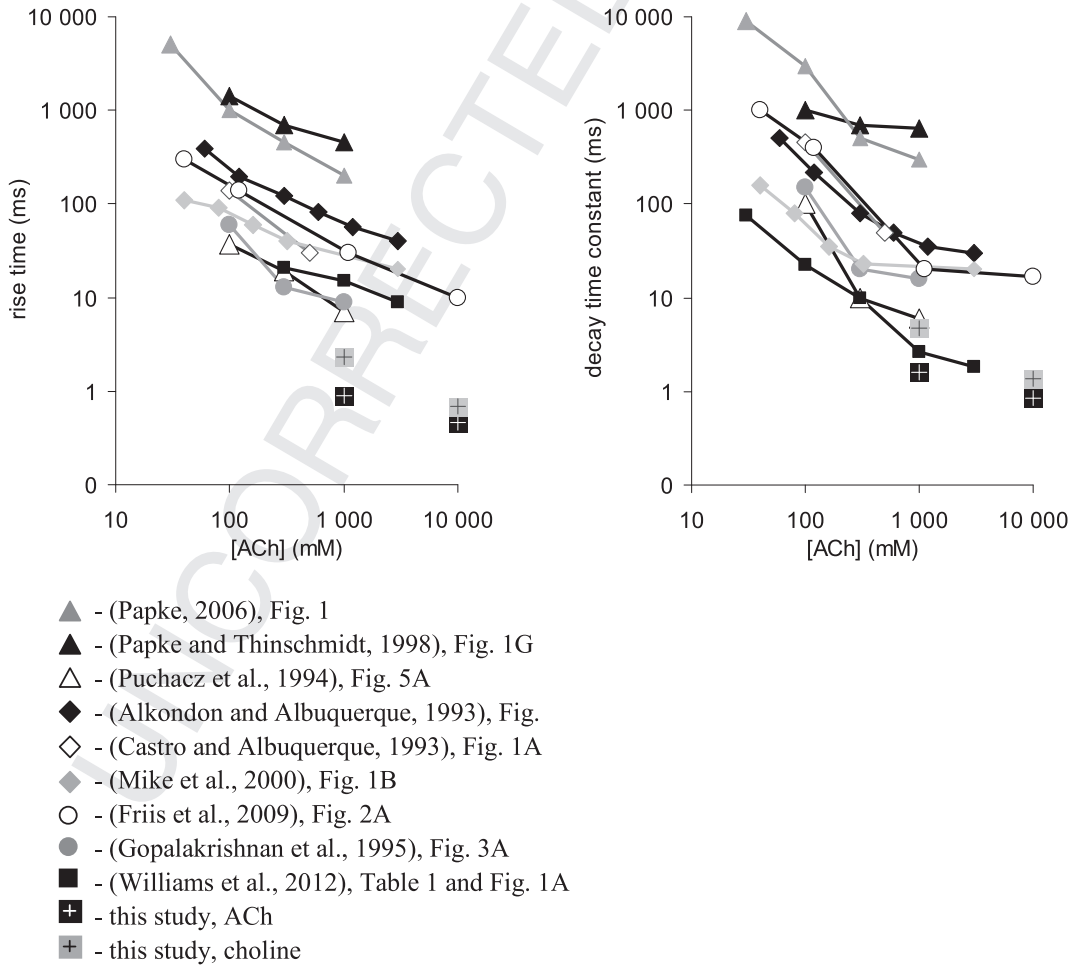

Fig. 1. Concentration-dependent kinetics of α7 nAChR-mediated currents. Concentration dependence of 10–90% current rise times (left panel), and decay time constants (right panel) obtained from 9 publications. Where data were not given numerically, they were measured using the figures of the publications. Figures illustrating concentration-dependence of ACh-evoked currents were enlarged, axes were adjusted to the calibration bar, and overlayed with exponential curves. Time constants were adjusted until the fit seemed adequate.

Please cite this article in press as: Pesti, K., et al., Kinetic properties and open probability of α7 nicotinic acetylcholine receptors, Neuropharmacology (2014), http://dx.doi.org/10.1016/j.neuropharm.2014.01.034

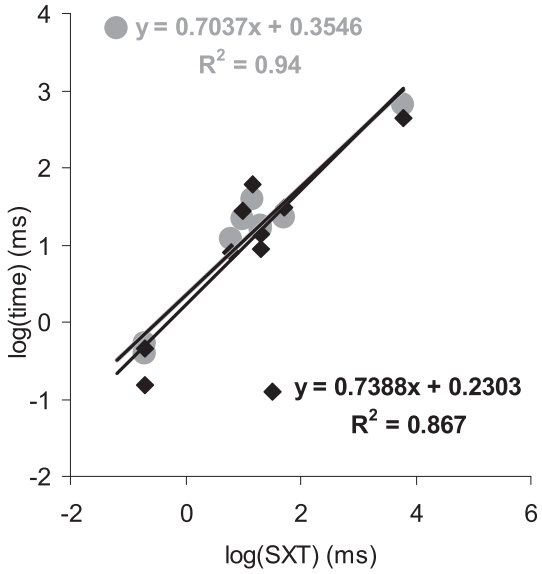

Fig. 2. Solution exchange rate-dependent kinetics of 1 mM ACh-evoked currents The logarithm of 10–90% rise times (black diamonds) and decay time constants (gray circles) are plotted against the logarithm of 10–90% solution exchange times (SXT). Data are from 9 papers (see text), including this study. Linear regression lines and coefficients of determination are shown.

receptors would detect the increase in agonist concentration, be activated and desensitized; consequently, the current would reach an identical peak and start decaying even before receptors could "learn" what final concentration would be to be applied. Therefore, the evoked currents would be identical (except for a minor difference in the late phase of the decay).

The explanation for this phenomenon is, that some of the gating transitions (opening, closing or desensitization) must be faster than the fastest experimentally tested solution exchange. When solution exchange is rate-limiting, it is natural that intrinsic gating of the receptor cannot be properly resolved.

Careful inspection of concentration-peak amplitude plots in the literature reveals that neither the increase in amplitude, nor the acceleration of kinetics could be saturated. The currents keep getting higher in amplitude and faster in kinetics even at supramaximal concentrations (i.e., which produce nearly full occupancy of binding sites at equilibrium) (up to 10 mM ACh (Friis et al., 2009)). It is typical in the literature that experimenters could not actually determine maximal amplitude, e.g. (Alkondon and Albuquerque, 1993; Khiroug et al., 2002; Papke, 2006; Puchacz et al., 1994; Williams et al., 2011), therefore maximal amplitudes are only extrapolated when concentration-peak amplitude plots are fitted with the Hill equation. This compromises the accuracy of determining EC_{50} values. (The situation is further complicated by the channel block caused by the agonist at high concentrations.)

In summary, both higher concentration with the same rate of solution exchange, and the same concentration with higher solution exchange rate provide a higher concentration gradient, and therefore evoke a faster current with higher amplitude. Because the rate of solution exchange thus far could not reach rates of receptor gating, the intrinsic kinetics of the receptor could not be resolved. The question of course is, how fast the solution exchange should be in order to appropriately record the intrinsic kinetics of the receptor.

Because of these properties, it is challenging to study α7 nAChRs. Even collecting simple concentration-response data is problematic: responses to individual concentrations are distorted by insufficiently fast solution exchange, and determination of the EC_{50} value is uncertain because of the difficulty in determining maximal current amplitude.

3.1.3. Aims of the investigation

In this study we attempted to address the following questions: Can we deduce the intrinsic kinetics of the receptor? How fast solution exchange would be required to resolve it experimentally?

We used two approaches to address these questions: extrapolation and simulation.

Although sufficiently fast solution exchange has been thus far unfeasible, we can examine the dependence of agonist-evoked current characteristics on solution exchange rate. From the solution exchange rate dependence of peak amplitude, rise time and decay time constant, these properties can then be extrapolated to instantaneous solution exchange.

Alternatively, a kinetic model can be constructed which reproduces both agonist concentration dependence and solution exchange rate dependence. Once we have a model like this, we can simulate any solution exchange rate, even if it is technically unfeasible, and can test the behavior of the channel even at instantaneous solution exchange. Here we encountered the problem of not having an adequate kinetic model. As we will describe in Section 3.3.1., none of the available models could correctly reproduce all kinetic properties of the receptor, therefore one of our aims was also to construct an improved model of the α7 nAChR.

3.2. Activation and desensitization kinetics of α7 nAChRs as measured using fast solution exchange

3.2.1. Properties of 10 mM choline-evoked currents

In most experiments we used choline as an agonist, because of its fast recovery (Mike et al., 2000), and its selectivity for α7 nAChRs. Normalized currents evoked by 10 mM choline are shown for whole cells and outside-out patches in Fig. 3. Eight cells, where currents were evoked by U-tube application are shown for comparison in Fig. 3A. The peak amplitude in these cells was −682 ± 126 pA (range: −325 to −1318 pA). The advantage of the U-tube system is that it can be used for cells attached to the culture dish. For the theta-tube, whole cells or outside-out patches were lifted to the mouth of the theta-tube. On the other hand, the theta tube was superior in the accuracy of the timing of drug pulses, and it could also provide somewhat faster solution exchange. For this reason in the rest of the experiments the theta tube was used for agonist perfusion. Currents evoked by theta-tube application are shown for 25 individual cells in Fig. 3B, left panel. The peak amplitude was −1300.4 ± 233.9 pA (median: −937 pA; range: −176 to −4511 pA). The distribution of amplitudes, and decay time constants plotted against 10–90% rise time values are shown in Fig. 3 middle and right panels, respectively. Whole-cell capacitances ranged from 2.0 to 13.9 pF (5.05 ± 0.49 pF), which corresponds to approximately 200–1400 μm^2 cell membrane surface (Hille, 1992), which means that the magnitude of current per membrane surface was −2.76 ± 0.48 pA/μm^2. Excision of patches always resulted in a drop in capacitance (<1 pF for all patches), in which range the accurate measurement of capacitance was not possible. While all cells were found to express functional α7 nAChRs, not all outside-out patches gave detectable agonist-evoked responses. Currents evoked by 10 mM choline ranged from 0 to 2675 pA. The mean current amplitude for all 68 patches was −137.9 ± 46.1 pA, the median was −14.85 pA. The distribution of amplitudes of currents evoked by theta-tube application of 10 mM choline both in whole-cell and outside-out mode are illustrated in Fig. 3D. In 28 Of the 68 patches no choline-evoked current was observed. In 17 patches the current was smaller than −50 pA, displaying discernible single channel events; from

Please cite this article in press as: Pesti, K., et al., Kinetic properties and open probability of α7 nicotinic acetylcholine receptors, Neuropharmacology (2014), http://dx.doi.org/10.1016/j.neuropharm.2014.01.034

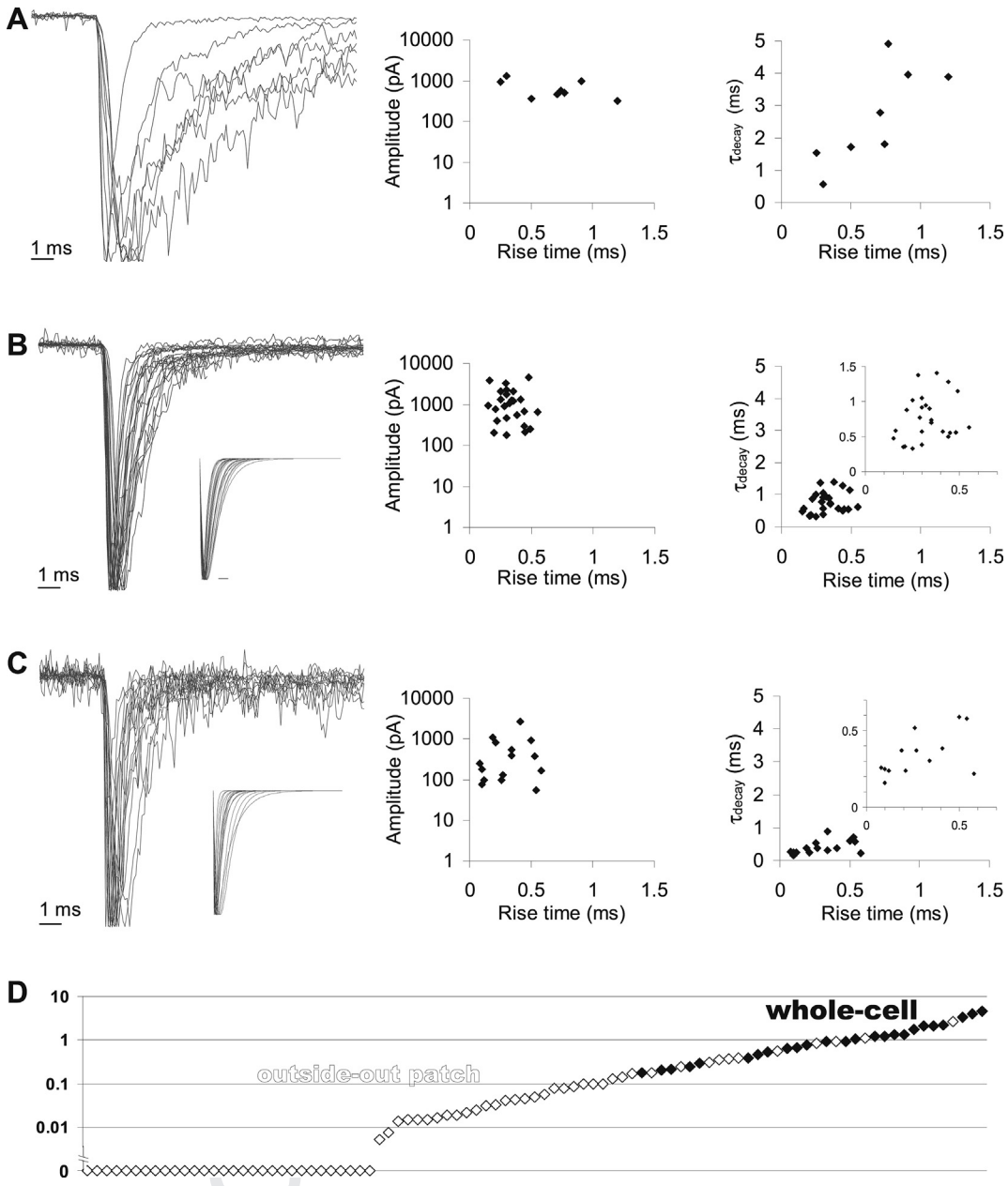

Fig. 3. Properties of 10 mM choline-evoked currents. Examples for normalized currents (left panel). Distribution of amplitudes (middle panel; on a logarithmic scale) and of decay time constants (right panel) are plotted against rise time (10–90%). Insets: The same plots on expanded scales. **(A)** Currents evoked by U-tube application on 8 cells. **(B)** Currents evoked by theta-tube application on 25 cells (whole-cell mode). **(C)** Currents evoked by theta tube application on 16 outside-out patches. Insets in the left panel of (**B**) and (**C**) show Bateman fits for the currents. **(D)** The distribution of all 25 whole-cell current amplitudes (closed diamonds) and all 68 outside-out patch current amplitudes (open diamonds).

these recordings we did not calculate rise times and decay time constants, for the sake of accuracy. In the rest of the patches ($n = 23$) the current was between −50 pA and −2675 pA. Currents recorded in 16 of these patches are shown in Fig. 3C. (In the other 7 patches 10 mM choline was given only in combination with PNU-120596, therefore, these were excluded from the analysis of current kinetics.) Distribution of rise times, amplitudes, and decay time constants are shown in the middle and right panels of Fig. 3C. The uneven distribution of current amplitudes in patches suggests clustering of receptors. The absence of observable choline-evoked current did not necessarily mean that the patch contained no receptors at all, because of the exceptionally low open probability of α7 nAChRs. Indeed, in the presence of PNU-120596 5 of the 28 non-responding patches became active, and showed choline-evoked currents. For whole-cell and outside-out recordings the average 10–90% rise time values were 0.41 ± 0.03 ms and 0.33 ± 0.03 ms; the average decay time constants were 0.94 ± 0.09 ms and 0.41 ± 0.04 ms, respectively. These results however should not be understood as true properties of the receptors, because the rate of solution exchange strongly affected current kinetics (as we discuss below). It is more appropriate to conclude based on the distribution of rise times and decay time constants (Fig. 3B and C), that both could be in the range of 0.1–0.4 ms.

Another way to assess kinetic properties of the receptor is to fit transition rate constants directly to the recordings. The simplest scheme for the interpretation of current rise and decay is the resting-open-desensitized chain of transitions (Bouzat et al., 2008; Papke, 2010), in which we disregard closing.

Please cite this article in press as: Pesti, K., et al., Kinetic properties and open probability of α7 nicotinic acetylcholine receptors, Neuropharmacology (2014), http://dx.doi.org/10.1016/j.neuropharm.2014.01.034

$$R \xrightarrow{o} O \xrightarrow{d} D$$ Scheme 1

This means that only two rate constants (opening "o" and desensitization "d") determine the shape of the current, and the process is described by the Bateman function (see Methods). If we fit our experimentally acquired currents with the Bateman function we can obtain apparent rate constants of opening and desensitization. These of course do not reflect individual transition rates of real receptors, but are products of association, dissociation, opening, closing and desensitization reactions. Nevertheless, the apparent rate constants can be used to characterize current kinetics. The two apparent rate constants were 2561 ± 243 s^{-1} and 2111 ± 146 s^{-1} for whole-cell currents, and 7594 ± 1982 s^{-1} and 2710 ± 441 s^{-1} for outside-out patches. Bateman functions fitted to the currents are shown in the insets of Fig. 3B and C. Note that the rise time and decay time constant of currents described by the Bateman function is insensitive to whether the opening or the desensitization rate constant is the higher: if the values of the two rate constants in Scheme 1 are swapped, only the amplitude and not the kinetics changes (Papke, 2010). For this reason we cannot attribute one apparent rate constant to the activation and the other to the desensitization, or vice versa. As we have discussed above, it is misleading to understand these values as mean properties of the receptors, because solution exchange times varied between individual patches, and currents which were evoked by slower agonist application are more distorted. The more appropriate conclusion is (as we discussed above for rise times and decay time constants), that apparent rate constants could be at least in the range of 2000 s^{-1}–8000 s^{-1}, which still might be an underestimation due to insufficient solution exchange rate.

Although the currents rapidly decayed approaching the baseline, they did not completely disappear in the continued presence of agonists, as it has been observed before (Mike et al., 2000; Uteshev et al., 2002). In the presence of 10 mM of choline a definite plateau phase (or "slow current" (Uteshev et al., 2002)) was observed, which was 1.16 ± 0.7% of the peak current. It was present in all cells (although in cells where the peak amplitude itself was small, we could not unambiguously determine its amplitude). At the termination of choline application no "rebound" current (Papke et al., 2000; Uteshev et al., 2002) was apparent, the current decayed to baseline with a time constant of 8.67 ± 0.92 ms.

Both unmodulated and PNU-120596-modulated choline-evoked currents were fully inhibited by 10 nM Methyllycaconitine ($n = 7$, data not shown).

3.2.2. *Dependence of choline-evoked current properties on solution exchange rate*

As we have discussed, the amplitude and kinetics of currents is distorted by insufficient solution exchange rate. To assess the extent of this distortion, we performed experiments in which solution exchange rate was modified. Our aim was to see if we could deduce the intrinsic kinetics of the receptor. We intended to achieve this by two approaches: extrapolation and modeling. On one hand, by recording currents evoked by different agonist exchange rates, we can extrapolate the properties (rise time, decay time constant and amplitude) of evoked currents to instantaneous solution exchange. On the other hand, we can construct a kinetic model of the receptor, which is able to reproduce the major characteristics of gating (including the exchange rate-dependence of current properties), and we can simulate instantaneous solution exchange. This second approach is described in Section 3.3.4.

A typical recording where different solution exchange rates were used is shown in Fig. 4A. Solution exchange rates for individual measurements were determined using open-tip junction potential measurement right after the experiments, without moving the pipette. Using the fastest voltage ramp to drive the piezoelectric device 10–90% solution exchange time (in the following text "10–90% solution exchange time" will be abbreviated as "SXT") values ranged from 0.23 to 0.55 ms depending on the geometry of the theta tube and the position of the pipette. The solution exchange rate was then modified by decreasing the slope of voltage ramps, which resulted in exchange rates slowed down to 1–3 m SXT. Decelerated solution exchange resulted in a significantly decreased amplitude.

In the case of whole-cell measurements, open-tip calibration may underestimate the SXT that receptors at the surface of the cell encounter, because of the geometry of the cell, and also because of the unstirred layer in immediate contact with the cell. At high flow velocity (5–20 cm/s) and with small diameter cells, such as in our case, this is not expected to cause a major difference (Sachs, 1999), but we wanted to test experimentally the accuracy of calibration. Previously the fast channel blocker tetramethylpiperidine has been used to assess SXT (Uteshev et al., 2002). Instead of using a channel blocker, we took advantage of the fact that the agonists choline and ACh also cause channel block at high concentrations. The highest ratio of channel block was reached by 10 mM of ACh {Szabo, #171}, therefore we used this concentration for calibration. In the presence of both the agonist and the positive modulator PNU-120596 receptors re-open from desensitization, and produce prolonged opening. When we remove only the agonist, but not the modulator, channels are rapidly relieved from block, which is reversible upon re-addition of the agonist. Using the same protocol that we used for agonist application we removed and re-applied 10 mM ACh in the continuous presence of 10 μM PNU-120596. This whole-cell-10-mM-ACh-unblock-calibration was compared with open-tip-junction-potential-calibration in $n = 7$ cells. A typical example is shown in Fig. 4B. Junction potential calibration and unblock calibration did not differ significantly, however, rise time values of 10 mM ACh-evoked currents were significantly ($p < 10^{-4}$, $n = 7$) lower than SXT-s measured with either of the calibration methods: The 10–90% rise time for 10 mM ACh-evoked currents was 18.8 ± 2.6% of the SXT measured with 10 mM ACh unblock. The current already peaked when only 12.5 ± 1.9% of the receptors was relieved from block. This confirms the observation that at high agonist concentrations (*i.e.*, when agonist association is not rate limiting) channel gating is faster than solution exchange, and therefore the peak is reached even before the receptors could encounter the final concentration.

Amplitude values plotted against SXT values of the calibration currents are shown for 7 individual cells in Fig. 4C (gray lines). Amplitudes were normalized to the value measured at 1 ms SXT (linear extrapolation from the two neighboring data points). Linear fits predicted that at instantaneous solution exchange, the amplitude would be 1.48 ± 0.15 times (range: 1.08–2.10) the amplitude measured at 1 ms SXT. This value most probably underestimates the true value, because the dependence of amplitude on solution exchange is not likely to be linear. Significantly better fit was achieved using monoexponential functions (gray dotted lines in Fig. 4C), and the predicted factor was 2.08 ± 0.25 times (range: 1.32–3.27), meaning that at instantaneous solution exchange the amplitude would be 2.1 times higher than the current evoked by 1 ms SXT. Biexponential fitting caused only negligible further improvement. In contrast to linear fits, mono- and bi-exponential

Please cite this article in press as: Pesti, K., et al., Kinetic properties and open probability of α7 nicotinic acetylcholine receptors, Neuropharmacology (2014), http://dx.doi.org/10.1016/j.neuropharm.2014.01.034

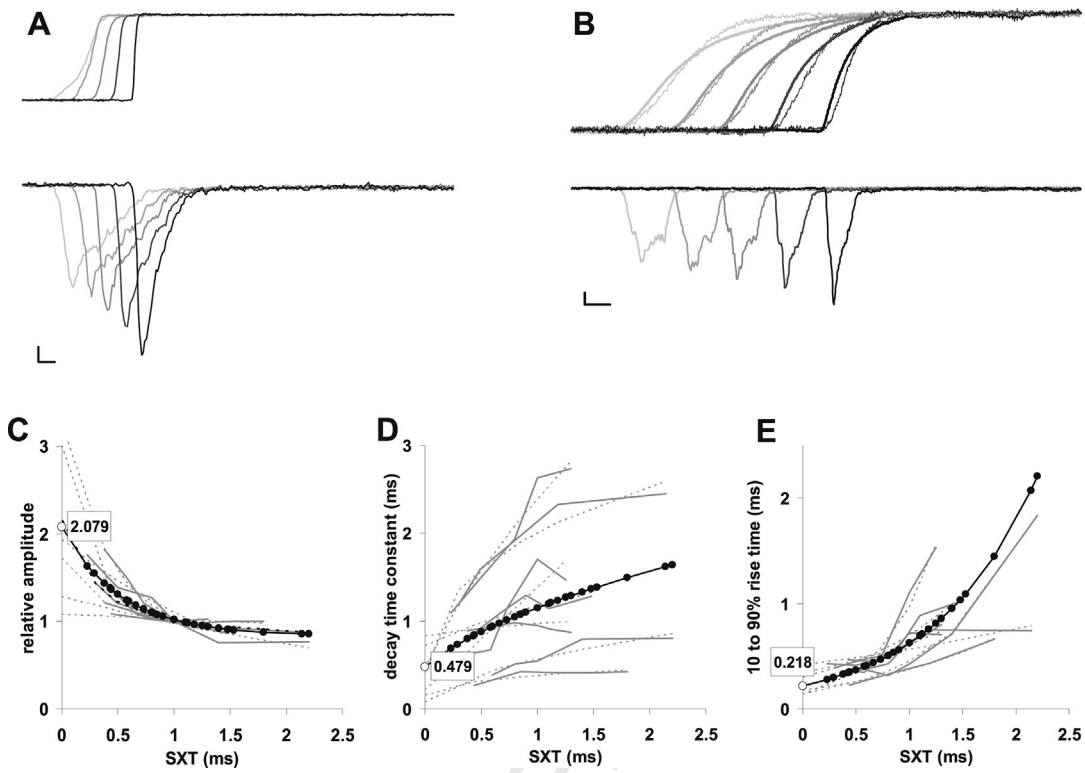

Fig. 4. Dependence of agonist-evoked current shape on solution exchange rate. **(A)** An example for the solution exchange rate, and the evoked currents. Scale bar: 100 pA, 1 ms. Successive traces are shifted by 1 ms for clarity. Upper panel: Open-tip junction potential measurements were used to measure solution exchange rate, SXT values in this experiment were 2.3, 1.3, 1.0, 0.6 and 0.35 ms; from light gray to black line. (Currents were scaled for visibility.) Lower panel shows corresponding 10 mM choline-evoked currents. **(B)** An example for the two calibration methods. Scale bar: 100 pA, 1 ms. Successive traces are shifted by 2 ms for clarity. Thick lines: open-tip-junction-potential-calibration, thin lines: 10-mM-ACh-unblock-calibration (co-application of 10 mM ACh and 10 μM PNU-120596 switched to application of 10 M PNU-120596 alone, upon which the channels are relieved from block caused by ACh). Both calibration curves were normalized for the sake of comparability. Lower panel shows corresponding 10 mM ACh-evoked currents. **(C–E)** Plots of 10 mM choline-evoked peak current amplitudes (**C**), decay time constants (**D**), and rise times (**E**) against 10–90% solution exchange times for 7 individual cells (gray lines). Dotted lines show fits by exponential (**C** and **E**) and power (**D**) functions. Individual parameters of the fitted equations were averaged, and the mean of each parameter was used to construct the equation that was used for extrapolation (black dotted lines). Open circles indicate the *y* axis intersection, with its value shown.

fits are likely to overestimate the amplitude at 0 SXT, because the amplitude is not expected to rise further, once the solution exchange rate has exceeded the intrinsic gating kinetics of the receptor. Values of the three parameters of monoexponential equations (see Section 2.5) fit to individual measurements were averaged, and the resulting equation is plotted on the figure (black line). It intersects the *y* axis at 2.08, which was essentially the same value that we got as the arithmetic mean of the seven individual values at 0 SXT.

Decay time constants for instantaneous agonist applications were extrapolated in a similar way (Fig. 4D). For linear extrapolation, the predicted decay time constants at 0 SXT ranged between 0.15 and 0.86 ms (0.52 ± 0.16 ms). The extrapolation predicted that instantaneous application would evoke a current where the decay time constant is 56.1 ± 10.2% of the time constant measured at 1 ms SXT. Using a power function (gray dotted lines in Fig. 4D) produced a better fit, and predicted similar decay time constants (0.41 ± 0.12 ms, ranging between 0.16 and 0.83 ms), but a somewhat larger difference between 0 ms and 1 ms SXT: the former was predicted to be 36.4 ± 10.4% of the latter. Besides individual measurements (gray lines) we also show the curve obtained by least squares fitting to all points (black line in Fig. 4D). It predicted a decay time constant of 0.48 ms at 0 ms SXT, which was 41.6% of the value at 1 ms SXT.

The dependence of rise time on solution exchange rate also did not appear to be linear (Fig. 4E), this plot was fit with an exponential function. The rise time extrapolated for instantaneous solution exchange was 0.22 ± 0.03 ms (range: 0.14–0.34 ms). The extrapolation predicted that at instantaneous exchange the rise time is 37.4 ± 5.6% of the value at 1 ms SXT.

We supposed that solution exchange rate can only be rate limiting when agonist association is fast enough. To test this, we conducted experiments in which the SXT-dependence of 1 and 10 mM of choline, as well as 1 and 10 mM of ACh were compared using the same cell ($n = 5$). As expected, 1 mM choline evoked slower currents with lower amplitude, the kinetics and amplitude of 1 mM ACh-evoked currents roughly matched those of 10 mM choline-evoked currents, and 10 mM ACh evoked even faster currents with higher amplitude. Relative rise times (as compared to 10 mM choline-evoked currents) for 1 mM choline, 1 mM ACh and 10 mM ACh were 4.00 ± 0.91, 1.14 ± 0.22, and 0.67 ± 0.07, respectively. Relative decay time constants were 3.87 ± 0.55, 1.22 ± 0.15, and 0.79 ± 0.11, while relative amplitudes 0.19 ± 0.02, 0.75 ± 0.06, and 1.54 ± 0.19. The SXT-dependence of 1 mM choline was nonsignificant within the 0.2–2.2 ms SXT range, 1 mM ACh-evoked currents showed SXT-dependence similar to 10 mM choline-evoked currents, while 10 mM ACh-evoked currents were the most SXT-dependent.

3.2.3. Recovery from desensitization

We have previously shown using U-tube agonist application that recovery from desensitization is rapid and agonist-dependent (Mike et al., 2000). However, this agonist application method is not ideal for quantitative measurement of recovery, because of the

Please cite this article in press as: Pesti, K., et al., Kinetic properties and open probability of α7 nicotinic acetylcholine receptors, Neuropharmacology (2014), http://dx.doi.org/10.1016/j.neuropharm.2014.01.034

considerable jitter in the delay of offset (up to 30 ms with U-tube application, while it was <0.2 ms for theta tubes). Using theta-tube agonist application, we measured recovery using short (180 ms) and long (5 s) pulses. We observed that recovery was somewhat delayed after the longer pulses, confirming the existence of more than one desensitized conformational states of α7 nAChRs (Uteshev et al., 2002; Wang et al., 2012; Williams et al., 2011), and similar observations using muscle-type (Elenes and Auerbach, 2002; Reitstetter et al., 1999) and α4β2 nAChRs (Paradiso and Steinbach, 2003). When high concentration of agonist is present for a prolonged period of time, receptors seem to reach a "deeper" desensitized state, from which recovery is slower. Recovery could only be adequately fitted by a bi-exponential function. The fast component was responsible for about half of the amplitude (55.8 ± 0.03% and 50.4 ± 0.04% for the short and long pulses, respectively) (Fig. 5). Time constants of recovery after short pulses were found to be 11.41 ± 3.23 and 308.6 ± 39.3 ms, while after long pulses 72.77 ± 18.84 and 1079.3 ± 106.3 ms ($n = 8$). For long pulses the fast time constant could not be accurately determined, because the shortest interpulse interval was 215 ms; bi-exponential fits gave adequate fits in the range of 10–100 ms. The slow time constant was, however, significantly higher than for the short pulses, no matter what the fast time constant was chosen to be ($p < 0.002$, $n = 8$). After the long pulses currents recovered only to 92.1 ± 3.1% of the control current, suggesting the existence of a third, even slower component of recovery. Least square fits to the averaged curves (shown in Fig. 5) gave 13.05 ms and 317.3 ms time constants for the recovery after short pulses, while 83.08 ms and 1073.9 ms for the recovery after long pulses.

The recovery was significantly slower, and could be adequately fitted with a monoexponential function, when the agonist was 300 μM nicotine. The time constants for the averaged curves were 505.7 ms and 1004 ms, for short and long pulses, respectively (Fig. 5).

3.2.4. Estimation of open probability

The number of receptors in individual outside-out patches was estimated using nonstationary fluctuation analysis. The method could not be used for the analysis of currents evoked by the agonist alone for a number of reasons: First, the rapid kinetics (most of the activity is over within a few milliseconds) would limit the number of samples collected for the analysis. Second, because of the extremely short open time a significant fraction of openings would escape detection, and thus part of the variance would be lost due to filtering. Finally, in the presence of the agonist the amplitude would be distorted by channel block. However, when the agonist is co-applied with PNU-120596, the open times are drastically prolonged, and a long (~1 s) tail current occurs after termination of agonist and modulator perfusion (Fig. 6). During this tail current the variance is not distorted by channel block (see accompanying paper for a more detailed discussion), open times are long, therefore the variance is not compromised by sampling rate and filtering, and sufficient number of samples can be collected for analysis. We first determined single channel conductance by making an all-point amplitude histogram from the final part of the decay, and fitting a sum of Gaussians on the histogram. This made our analysis more reliable, because we needed to determine only one of the two variables from the amplitude-variance plot. This compensated for the fact that the number of consecutively evoked currents used in the analysis was limited, because we could only use experiments where the current amplitude was stable. The absence of run-down was verified by stability plots for the currents: data where R^2 values between time and current amplitude exceeded 0.015 were excluded from analysis. Single channel amplitude was found to be 6.24 ± 0.17 pA at −70 mV holding potential. This means a conductance of 89.1 pS, and is in agreement with conductance values of α7 nAChRs activated by agonists in the presence of PNU-120596 (daCosta et al., 2011; Gusev and Uteshev, 2010; Kalappa et al., 2010), or by agonists alone (Castro and Albuquerque, 1993; Fucile et al., 2002; Mike et al., 2000; Valles et al., 2009). It has been observed recently, that single-channel amplitudes of currents evoked in the presence of the positive allosteric modulator TQS did not exactly match the amplitudes of currents evoked by the agonist alone, but were larger by 21.5%. This may likely be the case for PNU-120596 as well, although a statistically significant difference has not been thus far shown (daCosta et al., 2011; Hurst et al., 2005; Williams et al., 2011). The number of receptors was determined by fitting the amplitude-variance plots in 5 outside-out patches, using 21–34 consecutively evoked currents. From the number of receptors per patch we could conclude that the maximal amplitude reached in the presence of 10 mM choline and 10 μM PNU-120596 corresponded with 59.9 ± 5.75% of the channels being open simultaneously, while at the peak of 10 mM choline-evoked currents (using SXT ~1 ms) only 3.3 ± 0.6% of the channel population was open (supposing equal single channel conductance for choline-evoked and choline plus PNU-120596-evoked currents). Even if we suppose a non-equal single channel conductance, the peak open probability would not be higher than ~4%.

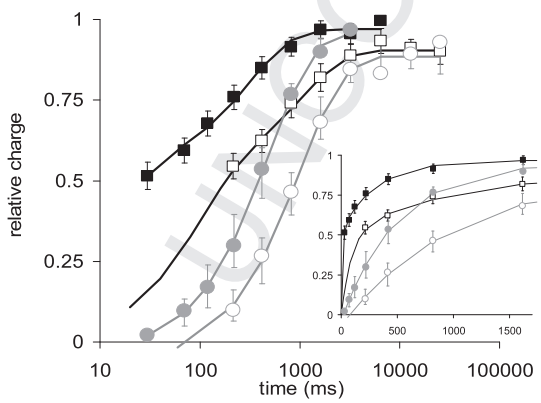

Fig. 5. Time course of recovery after 10 mM choline (black squares), and 300 μM nicotine (gray circles) application. Lines show bi-exponential (choline), and mono-exponential (nicotine) fits. Closed symbols: recovery after short agonist application (180 ms). Open symbols: recovery after long agonist application (5 s). The inset shows the same curves plotted against the initial 1600 ms of interpulse intervals on a linear time scale.

3.3. Interpretation of experimental data in the context of a kinetic model

3.3.1. The necessity of an improved kinetic model of the α7 nAChR

In order to reach a more thorough understanding of the intrinsic gating behavior of α7 nAChRs, and of the mechanism of action of the modulator PNU-120596 (see accompanying paper {Szabo, #171}), we needed an adequate model that could reproduce the major properties of the receptor.

Thus far three detailed kinetic models have been proposed (McCormack et al., 2010; Mike et al., 2000; Papke et al., 2000). We tested them by performing simulations in a number of experimental conditions. It was obvious that they do not only need a minor adjustment; we needed to construct a totally new model. Results of simulations in different experimental protocols are summarized in Table 1. Most importantly, none of the models was fast enough to reproduce gating kinetics as it is observed using submillisecond solution exchange (Bouzat et al., 2008), see also

Please cite this article in press as: Pesti, K., et al., Kinetic properties and open probability of α7 nicotinic acetylcholine receptors, Neuropharmacology (2014), http://dx.doi.org/10.1016/j.neuropharm.2014.01.034

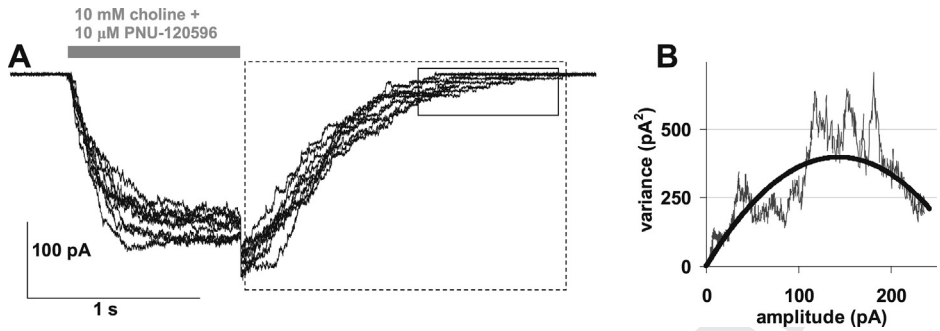

Fig. 6. Determination of the number of receptors in a patch using nonstationary fluctuation analysis. **(A)** An example for subsequent currents evoked by choline and PNU-120596. For the sake of clarity, only 10 of the total 34 traces are shown. The solid box indicates the region used for all-point histograms, the dotted box indicates the region used for nonstationary fluctuation analysis. **(B)** Amplitude variance plot of the decay phase of the current. Based on the least square fit of the quadratic function (thick line) $n = 52$ receptors were estimated in this patch.

Figs. 3 and 4 of this study. The following major characteristics of α7 nAChR-mediated currents were examined:

- Concentration-dependent amplitude and kinetics of evoked currents.
- Solution exchange rate-dependent amplitude and kinetics.
- Neither of these could be saturated, not even with agonist concentrations as high as 10 mM ACh (Friis et al., 2009), or solution exchange rates as fast as 0.1–1 m (Bouzat et al., 2008; daCosta et al., 2011; Williams et al., 2011).
- At high agonist concentration (1 mM ACh), and at submillisecond solution exchange (XCR = 0.5 ms), the rise time was ~0.1–0.3 ms, and the decay time constant was ~0.3–0.5 ms (Bouzat et al., 2008), and this current study (Figs. 3 and 4).
- Desensitization was almost complete even at lower concentrations. At high concentrations the plateau current amplitude was ~1% of the peak amplitude.
- The concentration-net-charge-flux plot differed from the concentration-peak amplitude plot in the following aspects: i) it had a lower EC_{50} value, ii) it had a higher slope, and iii) it had a definite plateau (Friis et al., 2009; Komal et al., 2011; Papke, 2006).
- Fast deactivation at the end of agonist application. No rebound current was seen at the end of agonist application with the two endogenous agonists.
- Recovery was fast and agonist-dependent.

Table 1 summarizes the performance of the three earlier models, and our current model. In the upper part of the table, we present numerical results of simulations. Italic fonts indicate results which are evidently unacceptable. The lower part summarizes the major qualitative features.

In summary, the Mike et al., 2000 model could not reproduce the low open probability, the McCormack et al., 2010 model produced currents that decayed very slowly, and the Papke et al., 2000 model showed no SXT-dependence, did not recover fast, and did not reproduce the concentration-net charge plot. The reason why the Mike et al., 2000 model could reproduce the low open probability, is in the topology of the model, which will be discussed in the next section.

3.3.2. Alternative topologies for the kinetic model

The three major states of the receptor that must be considered are resting, open and desensitized conformations. Bidirectional transition between any two of these states may be possible; therefore a general scheme that describes the receptor (at a certain agonist occupancy level) could be the following:

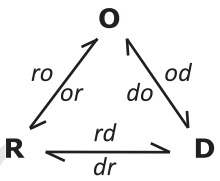

Scheme 2

where "*ro*" and "*or*" are the opening and closing rates, respectively; "*od*" and "*rd*" are rates of desensitization, "*do*" and "*dr*" are rates of recovery from desensitized state. Because there are redundant pathways of desensitization and recovery Scheme 2 can be simplified without losing the experimentally observed ability to open, close, desensitize and recover. There are two ways to simplify Scheme 2:

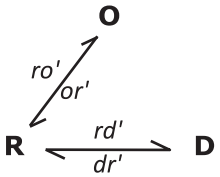

Scheme 3

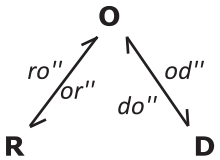

Scheme 4

Although we have used both the *R-O-D* (Mike et al., 2000) and the *O-R-D* (McCormack et al., 2010) topologies before, we have not systematically investigated if they are equally adequate for modeling this specific receptor. We tested their performance on a

Table 1
Summary of the three detailed kinetic models of α7 nAChRs from the literature, and our current model. Kinetic models were reconstructed, and simulations with the same protocols were run using all four models. Concentration-dependence of amplitude, kinetics and net charge flow was investigated, as well as SXT-dependence of kinetics and amplitude. Upper eight rows summarize main quantitative data, italic fonts indicate data that are evidently inappropriate. Lower 15 rows show most important qualitative properties.

Properties of simulated currents:	Model:			
	Mike et al., 2000	Papke et al., 2000	McCormack et al., 2010	Current study
EC_{50} concentration-peak amplitude plot (μM)	**112.8**	**79.6**	**122.7**	**306.7**
n_H concentration-peak amplitude plot	**1.45**	**2.40**	**1.53**	**1.48**
EC_{50} concentration-net charge plot (μM)	**7.07**	*76.7*	**64.8**	**11.81**
n_H concentration-net charge plot	**2.88**	*2.48*	*1.67*	**3.07**
peak p_{open}(1 mM ACh-evoked current, SXT = 2 ms)	*0.27*	**0.0029**	**0.018**	**0.025**
10–90% rise time (ms) (1 mM ACh, SXT = 2 ms)	**0.79**	**0.77**	**1.58**	**0.47**
τ_{decay} (ms)(1 mM ACh, SXT = 2 ms)	**1.20**	**0.74**	*108*	**0.23**
Amplitude ratio: SXT = 1.5 ms/SXT = 6 ms (1 mM ACh)	**1.82**	*0.68*	*1.04*	**4.95**
Concentration-dependent acceleration of onset	**Yes**	**Yes**	**Yes**	**Yes**
Concentration-dependent acceleration of decay	**Yes**	**Yes**	**Yes**	**Yes**
Low open probability	*No*	**Yes**	**Yes**	**Yes**
Almost complete desensitization at 100 μM ACh	**Yes**	*No*	**Yes**	**Yes**
Onset and decay kinetics fast enough	*No*	*No*	*No*	**Yes**
Concentration – net charge flux plot: lower EC_{50}	**Yes**	*No*	**Yes**	**Yes**
Concentration – net charge flux plot: higher slope	**Yes**	*No*	*No*	**Yes**
Concentration – net charge flux plot: reaches plateau	*No*	*No*	**Yes**	**Yes**
Concentration – peak amplitude plot: keeps increasing	**Yes**	*No*	**Yes**	**Yes**
Faster kinetics with faster solution exchange	**Yes**	**Yes**	**Yes**	**Yes**
Amplitude increases with faster solution exchange	**Yes**	*No*	*No*	**Yes**
Absence of rebound current	**Yes**	*No*	**Yes**	**Yes**
Fast recovery	*No*	*No*	*No*	**Yes**

simple transient current with kinetic parameters similar to experimentally acquired agonist-evoked currents.

In the triangular model we set "*do*" and "*dr*" to zero for the sake of simplicity (recovery is negligible in the presence of an agonist). We know that the mean open time is ~50 μs, therefore we constrained the model so that the sum of closing rates (*or* + *od*) was 20,000.

Thus we had three free parameters, "*ro*", "*rd*" and "*or*". We first intended to reproduce an agonist-evoked current using the triangular model, and then see if the simplified models can still produce the same current. In experiments (Fig. 3C) we saw that the rise time could be as fast as <100 μs, and the decay time constant as low as ~200 μs. Using the parameters $ro = 1000\ s^{-1}$, $or = 10{,}000\ s^{-1}$, $od = 10{,}000\ s^{-1}$, $rd = 5000\ s^{-1}$, the rise time was 67 μs, the decay time constant 212 μs, and the peak open probability 0.03 (which is similar to experimental data, as discussed below). We tried to reproduce this simulated current curve using the two simplified models, by fitting the simulated current curve produced by both simplified models to this one. The model with the O-R-D topology could exactly replicate the curve with the parameter values $ro = 1000\ s^{-1}$, $or = 20{,}000\ s^{-1}$ and $rd = 5000\ s^{-1}$. The R-O-D model, however, was unable to replicate the curve (Fig. 7A) (the kinetics itself could be exactly reproduced, but only when we allowed higher open probability). This is reasonable, because maximizing the open probability at 0.03 would mean that we try to force all receptors through a very narrow bottleneck. In fact even with the triangular topology this can only be done when the *ro*/*rd* ratio is low enough (it was 0.2 in this case). When we constrained the *ro*/*rd* ratio to be 0.25, 0.5 or 1, the current could not be replicated. Best fits to the same curve with the constraint of *ro*/*rd* = 0.25, 0.5 and 1 are shown in Fig. 7B.

In summary, in the case when fast kinetics of currents and low open probability coexist (such as in the case of the α7 nAChR), triangular topology can be simplified to the *O-R-D*, but not to the *R-O-D* topology. When either of these conditions is not required, both topologies are possible. Fig. 7C and D illustrate these cases. In Fig. 7C the *ro*/*rd* ratio was changed: $ro = 5000\ s^{-1}$ and $rd = 1000\ s^{-1}$. The resulting current with peak open probability = 0.16 could be reproduced with both *O-R-D* ($ro = 5580\ s^{-1}$, $rd = 3862\ s^{-1}$), and *R-O-D* ($ro = 4196\ s^{-1}$, $or = 2823\ s^{-1}$ and $od = 17{,}177\ s^{-1}$) models. Fig. 7D illustrates a simulated current with the same low open probability but slower kinetics: ($ro = 750\ s^{-1}$, $rd = 250\ s^{-1}$), and the curves produced by the simplified models fitted to it. The fitted parameters were: $ro = 763\ s^{-1}$, $rd = 635\ s^{-1}$ for the *O-R-D* topology, and $ro = 688\ s^{-1}$, $or = 1563\ s^{-1}$ and $od = 18436\ s^{-1}$ for the *R-O-D* topology.

In summary, considering the open probability and the kinetics of α7 nAChR-mediated currents evoked by high agonist concentration, we can conclude that the majority of receptors must desensitize from closed state. Therefore the *O-R-D* topology clearly represents α7 nAChRs better than the *R-O-D* topology.

We have one more reason for thinking that models with *O-R-D* topology might indicate the behavior of the receptor better. The mean channel open time was not found to depend on agonist occupancy (Bouzat et al., 2008; daCosta et al., 2011; Mike et al., 2000). This could be explained by supposing a single open state (Papke et al., 2000), but simulations with single-open-state-models produced concentration-response curves, which reach a maximum and then decay again, which is not what we observed experimentally. We could only reproduce acceptably concentration-response curves with multiple open state models. The observation that mean open times do not noticeably differ depending on the number of bound agonists, requires that in the model the sum of rate constant values for transitions leaving the open state is constant throughout all agonist occupancy levels. It is more prudent to suppose that *or'* in Scheme 3 is constant (does not depend on the number of bound agonist molecules), than to suppose that in Scheme 4, where "*od*" must radically increase at higher agonist occupancy levels, the parallel decrease in "*or*" just happens to exactly balance that.

3.3.3. Construction of the model of the α7 nAChR

The topology of the model is illustrated in Scheme 5. The differences compared to our previous models are: i) in order to better reproduce concentration-dependent kinetics and sensitivity to solution exchange rate, we included all six agonist occupancy levels

Please cite this article in press as: Pesti, K., et al., Kinetic properties and open probability of α7 nicotinic acetylcholine receptors, Neuropharmacology (2014), http://dx.doi.org/10.1016/j.neuropharm.2014.01.034

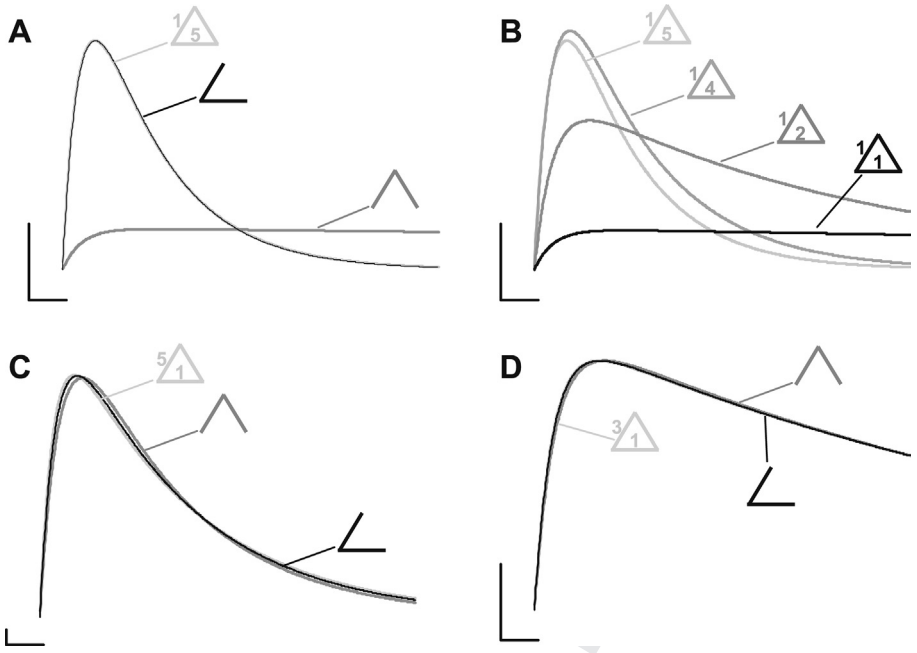

Fig. 7. Comparison of alternative topologies for the kinetic scheme. Schematic representation of topologies refer to Schemes 2–4. Small numbers indicate the ratios between *"ro"* and *"rd"* rate constants. Scale bars: 0.01 (open probability), 0.1 ms. **(A)** Fast-kinetics-low-open-probability simulated current produced by the triangular model (light gray line) could be fitted by the *O-R-D*, but not the *R-O-D* topology. **(B)** Importance of *"ro"–"rd"* ratio in triangular models. Light gray line shows the same simulated current shown in (A), with *ro/rd* = 0.2. Darker gray and black lines show *ro/rd* ratios: 0.25, 0.5 and 1, which were unable to reproduce fast-kinetics-low-open-probability simulated currents. **(C)** Fast-kinetics-high-open-probability simulated currents could be adequately reproduced by both simplified topologies. (Note the difference in the scale bar) **(D)** Slow-kinetics-low-open-probability simulated currents also could be reproduced by both alternative models.

(from 0 to 5), ii) we introduced a slow desensitized state ("S"), iii) we readjusted parameters to fit solution exchange rate-dependent kinetics. Including an additional desensitized state was also necessary in order to tackle the problem of PNU-120596-sensitive and insensitive desensitized states (Williams et al., 2011). We did not attempt to identify the number of distinct desensitized states, and to perform a kinetic characterization of each individual state. There are most probably more than only two distinct states, as it was found in muscle-type nAChRs (Elenes and Auerbach, 2002).

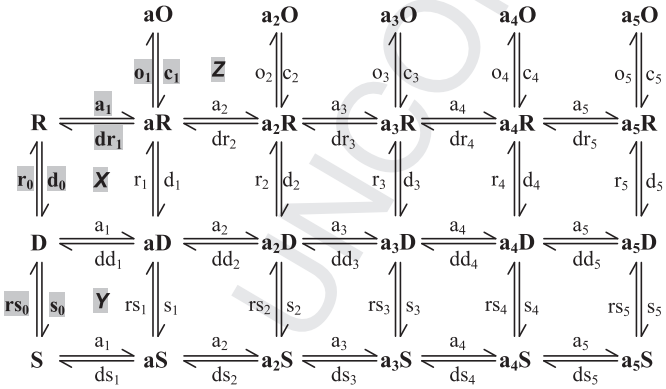

Scheme 5

The model is Monod–Wyman–Changeux type model, i.e., it is constructed in a way that the same constants (denoted "allosteric factors", *X* and *Y*) determine differences in affinity between different conformations and differences in gating equilibria between different agonist occupancy levels (*i.e.*, if desensitized conformation has an *X* times higher affinity than resting conformation, then binding of one agonist molecule increases the propensity of resting receptors to desensitize exactly *X*-fold). The constant *Z* determines only the changes in opening rates upon agonist association. Closing rates were chosen to be constant for all agonist occupancy levels, because mean open times were found to be similar at all agonist concentrations (Bouzat et al., 2008; daCosta et al., 2011; Mike et al., 2000). For the sake of simplicity, we used the same *X*, *Y* and *Z* factors for all five agonist binding steps. Using this principle the whole model can be built up using only 11 free parameters (shown in shaded bold fonts in Scheme 5). Values of parameters and calculation of rate constants are given in Table 2.

3.3.4. Simulated agonist evoked currents

Concentration-dependence of simulated currents is illustrated in Fig. 8A. The 10–90% solution exchange rate used in this simulation was 2 ms. The plateau phase and the deactivation after agonist application (the 'slow' and 'delayed' current component (Uteshev et al., 2002)) are shown in the inset on a 100× enlarged scale. Concentration-peak amplitude and concentration-net charge plots are shown in Fig. 8B, together with the Hill equation fits. For peak amplitudes the values of best fit were EC_{50} = 1236 μM, n_H = 1.61, for net charge EC_{50} = 134.6 μM, n_H = 2.30. The concentration dependence of rise times and decay time constants (Friis et al., 2009; Gopalakrishnan et al., 1995; Mike et al., 2000; Papke and Thinschmidt, 1998) were qualitatively reproduced, as well as the plateau current and the decay after the end of agonist application. We did not aim to fit parameters to the exact quantitative properties of experimentally measured currents, because that would have required adjustment of several unknown parameters. For example, allosteric factors *X*, *Y* and *Z* are most likely not constant for each agonist binding step. It has been proposed that at medium levels of agonist occupancy receptors favor opening, while

Table 2
Rate constants (left column), their calculation (middle column) and their values (right column) for Scheme 5. Rate constants are in s^{-1} units, with the exception of association rates (a1–a5), which are in s^{-1} μM^{-1} units. Free parameters are in bold font.

X		**5**
Y		**2**
Z		**20**
a1		50
a2	=a1*4/5	40
a3	=a1*3/5	30
a4	=a1*2/5	20
a5	=a1/5	**10**
dr1		**5000**
dr2	=dr1*2	10000
dr3	=dr1*3	15000
dr4	=dr1*4	20000
dr5	=dr1*5	25000
dd1	$=dr1/X^2$	200
dd2	$=dr2/X^2$	400
dd3	$=dr3/X^2$	600
dd4	$=dr4/X^2$	800
dd5	$=dr5/X^2$	1000
ds1	$=dd1/Y^2$	50
ds2	$=dd2/Y^2$	100
ds3	$=dd3/Y^2$	150
ds4	$=dd4/Y^2$	200
ds5	$=dd5/Y^2$	250
o1		**0.05**
o2	=o1*Z	1
o3	$=o1*Z^2$	20
o4	$=o1*Z^3$	400
o5	$=o1*Z^4$	8000
c1-5		20 000
d0		**5**
d1	=d0*X	25
d2	$=d0*X^2$	125
d3	$=d0*X^3$	625
d4	$=d0*X^4$	3125
d5	$=d0*X^5$	15625
r0		**5000**
r1	=r0/X	1000
r2	$=r0/X^2$	200
r3	$=r0/X^3$	40
r4	$=r0/X^4$	8
r5	$=r0/X^5$	1.6
s0		**0.02**
s1	=s0*Y	0.04
s2	$=s0*Y^2$	0.08
s3	$=s0*Y^3$	0.16
s4	$=s0*Y^4$	0.32
s5	$=s0*Y^5$	0.64
rs0		**1**
rs1	=rs0/Y	0.5
rs2	$=rs0/Y^2$	0.25
rs3	$=rs0/Y^3$	0.125
rs4	$=rs0/Y^4$	0.0625
rs5	$=rs0/Y^5$	0.03125

at high levels they favor desensitization (Papke et al., 2000). This mechanism could be approached by defining agonist occupancy level-dependent allosteric factors. However, the current model showed that all major properties of the behavior of α7 nAChRs could be qualitatively reproduced with this simple 11-free-parameter-model. Pulse duration-dependent changes in recovery rate suggest that S states are somewhat more absorbing than D states, and the slow kinetics suggests that a high energy barrier must be constructed for the D to S transition. Our parameters as shown in Table 1 qualitatively reproduced bi-exponential, pulse duration-dependent recovery kinetics. Solution exchange rate dependence is shown in Fig. 8C. We found a dependence that was similar to experimental observations. Instantaneous application of 10 mM choline produced simulated currents with 0.133 ms rise time (10–90% time was 0.072 ms), and the decay time constant was 0.288 ms. We asked the question how much an experimentally observed current is distorted. In Fig. 8D we plotted the properties of simulated currents on the figures of experimental data (the same data as shown in Fig. 4C–E). We show simulations of 10 mM choline-evoked currents at SXTs: 0.016, 0.031, 0.063, 0.125, 0.25, 0.5, 1 and 2 ms. When we compared simulated currents evoked by quasi-instantaneous (0.016 ms) solution exchange "(Inst)", to a 1 ms SXT "(1 ms)", amplitude (Inst) was 2.00 times higher than amplitude (1 ms). This is similar to the value (2.08 times higher) we obtained by extrapolation using exponential equations. We could observe that solution exchange faster than about 60–80 μs did not cause further significant change in current characteristics. We found the decay time constant to be less sensitive to solution exchange rate in simulations (Fig. 8D): The decay time constant (Inst) was 79.3% of τ(1 ms) in simulations, while the extrapolated τ(Inst) was 41.6% of the experimental τ(1 ms). Overestimation of the rise time was estimated to be similar by simulations and extrapolation: rise time (Inst) was estimated to be 35.1% and 37.4%, respectively (Fig. 8D). In order to summarize the prediction by simulation and extrapolation in a straightforward manner, we illustrate the 10 mM choline-evoked simulated current at 1 ms SXT and at 0.016 ms (quasi-instantaneous) SXT, as well as a simulated current, where the parameters were adjusted to match the amplitude and kinetics predicted by extrapolation to instantaneous solution exchange.

The simulations also gave an estimation on how fast the solution exchange should be in order to correctly resolve the intrinsic kinetics of the receptor. Using our current parameters (Table 1), 60–80 μs SXT was sufficiently fast, which means that recording of undistorted intrinsic kinetics is experimentally attainable (Auzmendi et al., 2012; Liu and Dilger, 1991; Sachs, 1999).

As we have discussed in Section 3.2.2., at lower concentrations the SXT dependence was weaker, and (at 100 μM choline it vas virtually absent). On the other hand, 10 mM ACh-evoked currents were more SXT dependent. The reason for this could be that at lower concentrations, instead of solution exchange rate, association rate becomes rate limiting. In general, at low agonist concentrations undistorted currents could be evoked by slower solution exchange, while high concentrations evoked currents which were more strongly SXT-dependent. This situation led to a curious phenomenon: Simulated concentration-peak amplitude curves diverged at higher concentrations (Fig 8F), which produced an apparent shift of EC_{50} values depending on SXT on normalized concentration-peak amplitude curves: with faster solution exchange the affinity of the agonist appeared to decrease (Fig. 8G). Concentration-net charge plots, on the other hand, were essentially insensitive to solution exchange rate in the range of 2–20 ms SXT (Fig. 8H).

4. Conclusions

A review of the literature of α7 nAChR-mediated currents indicates that measured kinetics is distorted by limited solution exchange time, in fact the kinetic parameters reflect properties of the solution exchange system much more that the genuine properties of receptors. We propose that peak amplitudes do not reflect the concentration of the agonist perfused, but rather the slope of agonist concentration increase at the beginning of agonist application, From this it follows that maximal peak amplitude cannot be reached in concentration-response experiments, and therefore EC50 values of agonists are bound to be inaccurate. This raises the question, whether the intrinsic kinetic properties of α7 nAChRs can be determined, how fast solution exchange would be needed to accomplish this, and what the EC50 values in such case would be. These problems also challenged us to construct a kinetic model of α7 nAChRs, which could reproduce major characteristics of

Please cite this article in press as: Pesti, K., et al., Kinetic properties and open probability of α7 nicotinic acetylcholine receptors, Neuropharmacology (2014), http://dx.doi.org/10.1016/j.neuropharm.2014.01.034

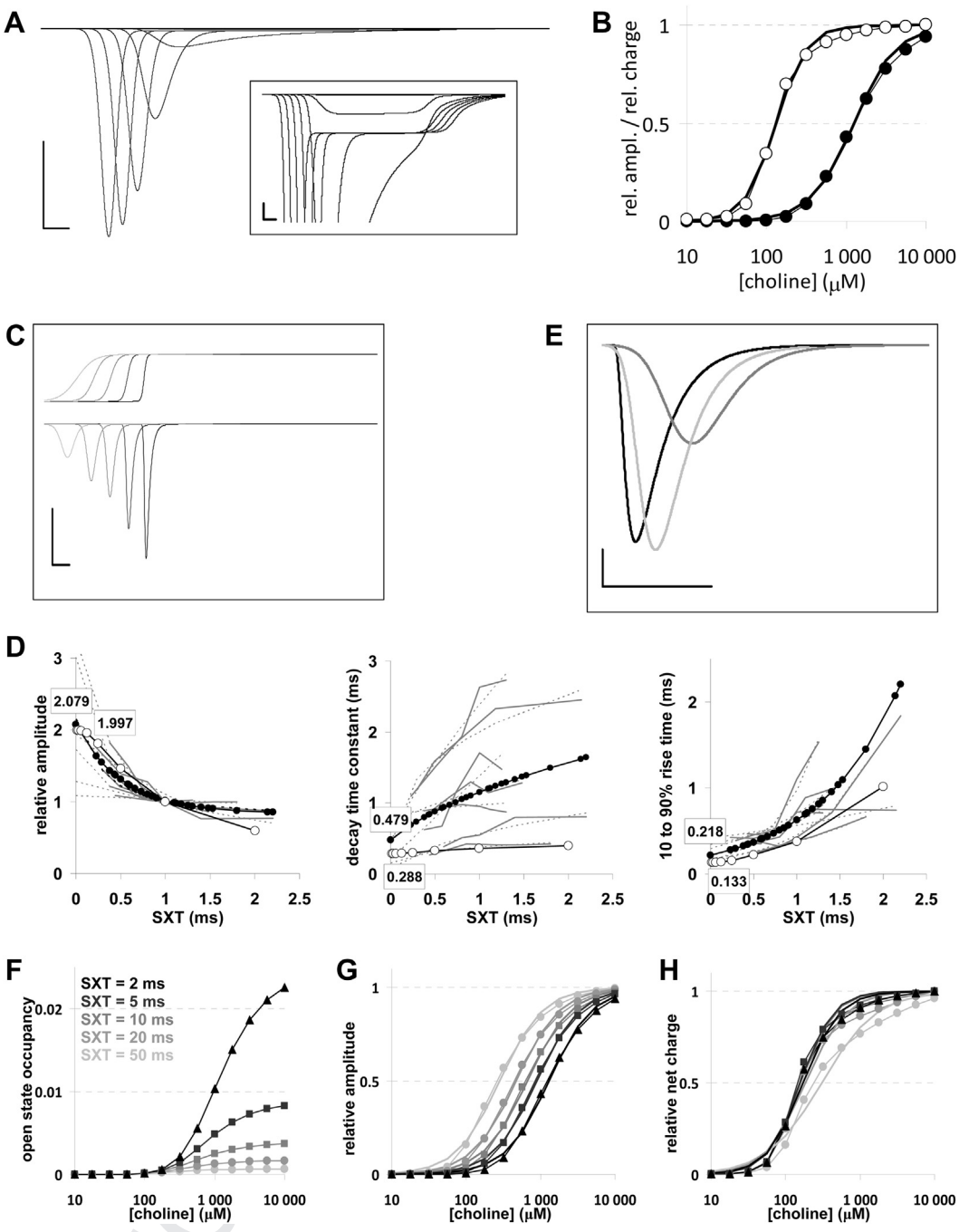

Fig. 8. Simulated currents using the model shown in Scheme 5. **(A)** Currents evoked by 10, 31.62, 100, 316.2, 1000, 3162, 10000 and 31623 μM choline. Scale bar: 1 ms, 0.01 (fraction of receptors in open states). Inset shows the same simulated currents on a hundred-fold enlarged scale. Scale bar: 1 ms, 0.0001 (fractional occupancy of open states). **(B)** Concentration-peak amplitude (filled symbols) and concentration-net charge (open symbols) plots made from the currents shown in (A). Thick lines indicate Hill equation fits on the data. **(C)** Solution exchange rate-dependence of current kinetics and amplitude. Solution exchange rates (upper traces) were chosen to reproduce those shown in Fig. 4. SXT values were 2.3, 1.3, 1, 0.6 and 0.35 ms (from light gray to black). Lower traces show simulated currents (occupancy of open states). Currents were shifted by 1 ms for visibility. Scale bar: 1 ms, 0.01 (fractional occupancy). **(D)** Relative amplitude, rise time and decay time constant values of simulated currents, plotted against SXT, shown together with corresponding experimental data (see Fig. 4C–E). **(E)** Simulated currents evoked by 1 ms SXT (dark gray line), and by quasi-instantaneous (SXT = 0.016 ms) solution exchange (black line), as well as reconstruction of the current predicted by extrapolation (light gray line). **(F)** SXT-dependence of concentration-peak amplitude curves. The maximal occupancy of all open states was plotted against choline concentration, when agonist application with five different SXTs were simulated. **(G)** SXT-dependence of normalized concentration-peak amplitude curves. **(H)** SXT-dependence of normalized concentration-net charge curves.

experimentally studied receptors, and which might provide an insight into their operation.

In this study we attempted to deduce the intrinsic kinetics of α7 nAChRs, and to refine existing kinetic models used for simulation of receptor behavior. Based on the experiments and simulations, we propose the following major conclusions:

From our simulations we propose that a ~60–80 μs SXT (10–90% solution exchange time) would be required to acceptably resolve intrinsic receptor kinetics when 10 mM choline is used as an agonist. In general, higher agonist concentrations require shorter SXT. Our experiments and simulations suggest that at 1 ms SXT 1 mM choline-evoked currents fairly well represent the

Please cite this article in press as: Pesti, K., et al., Kinetic properties and open probability of α7 nicotinic acetylcholine receptors, Neuropharmacology (2014), http://dx.doi.org/10.1016/j.neuropharm.2014.01.034

intrinsic kinetics of the receptor, while 10 mM choline-evoked currents are remarkably distorted: Compared to 1 ms SXT, instantaneous solution exchange would evoke a current which has an amplitude ~2× higher (reaching a peak open probability of ~0.07), a rise time ~2.7 times shorter (~0.1–0.2 ms), and a decay time constant ~1.25–2.7 time lower (0.2–0.5 ms).

Using theta tubes allowed determination of the recovery rate with much more accuracy, than U-tube application in a previous study on native receptors (Mike et al., 2000). Within 1 s the recovery was essentially complete after a short pulse of choline. The recovery, however, was both agonist-dependent, suggesting that agonist dissociation was rate limiting; and pulse duration-dependent, which confirmed the presence of more than one desensitized states.

Currents evoked by 10 mM choline, with ~1 ms SXT, evoked a current with peak open probability of 0.033, a uniquely low value among receptor ion channels. In the presence of 10 μM PNU-120596, open probability could be as high as 0.6.

A comparative simulation study of published kinetic models showed that the model we describe in this study is the first kinetic model that can adequately reproduce low open probability, fast kinetics, fast recovery and solution-exchange-rate-dependent kinetics, as these properties are observed experimentally. By simulations we also provided evidence that at high agonist concentration the majority of the receptor population must reach desensitized state without prior opening.

Uncited references

Mike et al., .

Acknowledgment

The pCEP4/rat α7 nAChR expressing GH4C1 cell line was kindly provided by Siena Biotech S.p.A. (Siena, Italy). This work was supported by grant NK72959 from the Hungarian Research Fund (OTKA) and by the Project Based Personnel Exchange Program of the Hungarian Scholarship Board (MÖB) and the German Academic Exchange Service (DAAD).

References

Albuquerque, E.X., Pereira, E.F., Alkondon, M., Rogers, S.W., 2009. Mammalian nicotinic acetylcholine receptors: from structure to function. Physiol. Rev. 89, 73–120.

Alkondon, M., Albuquerque, E.X., 1993. Diversity of nicotinic acetylcholine receptors in rat hippocampal neurons. I. Pharmacological and functional evidence for distinct structural subtypes. J. Pharmacol. Exp. Ther. 265, 1455–1473.

Alkondon, M., Albuquerque, E.X., 2001. Nicotinic acetylcholine receptor alpha7 and alpha4beta2 subtypes differentially control GABAergic input to CA1 neurons in rat hippocampus. J. Neurophysiol. 86, 3043–3055.

Auzmendi, J., Fernandez Do Porto, D., Pallavicini, C., Moffatt, L., 2012. Achieving maximal speed of solution exchange for patch clamp experiments. PLoS One 7, e42275.

Bouzat, C., Bartos, M., Corradi, J., Sine, S.M., 2008. The interface between extracellular and transmembrane domains of homomeric Cys-loop receptors governs open-channel lifetime and rate of desensitization. J. Neurosci. 28, 7808–7819.

Castro, N.G., Albuquerque, E.X., 1993. Brief-lifetime, fast-inactivating ion channels account for the alpha-bungarotoxin-sensitive nicotinic response in hippocampal neurons. Neurosci. Lett. 164, 137–140.

daCosta, C.J., Free, C.R., Corradi, J., Bouzat, C., Sine, S.M., 2011. Single-channel and structural foundations of neuronal {alpha}7 acetylcholine receptor potentiation. J. Neurosci. 31, 13870–13879.

Elenes, S., Auerbach, A., 2002. Desensitization of diliganded mouse muscle nicotinic acetylcholine receptor channels. J. Physiol. 541, 367–383.

Fedorov, N., Benson, L., Graef, J.D., Hyman, J., Sollenberger, J., Pettersson, F., Lippiello, P.M., Bencherif, M., 2012. A method for bidirectional solution exchange–"liquid bullet" applications of acetylcholine to alpha7 nicotinic receptors. J. Neurosci. Methods 206, 23–33.

Franke, C., Hatt, H., Dudel, J., 1987. Liquid filament switch for ultra-fast exchanges of solutions at excised patches of synaptic membrane of crayfish muscle. Neurosci. Lett. 77, 199–204.

Friis, S., Mathes, C., Sunesen, M., Bowlby, M.R., Dunlop, J., 2009. Characterization of compounds on nicotinic acetylcholine receptor alpha7 channels using higher throughput electrophysiology. J. Neurosci. Methods 177, 142–148.

Fucile, S., Palma, E., Martinez-Torres, A., Miledi, R., Eusebi, F., 2002. The single-channel properties of human acetylcholine alpha 7 receptors are altered by fusing alpha 7 to the green fluorescent protein. Proc. Natl. Acad. Sci. U.S.A. 99, 3956–3961.

Gopalakrishnan, M., Buisson, B., Touma, E., Giordano, T., Campbell, J.E., Hu, I.C., Donnelly-Roberts, D., Arneric, S.P., Bertrand, D., Sullivan, J.P., 1995. Stable expression and pharmacological properties of the human alpha 7 nicotinic acetylcholine receptor. Eur. J. Pharmacol. 290, 237–246.

Gray, R., Rajan, A.S., Radcliffe, K.A., Yakehiro, M., Dani, J.A., 1996. Hippocampal synaptic transmission enhanced by low concentrations of nicotine. Nature 383, 713–716.

Gu, Z., Yakel, J.L., 2011. Timing-dependent septal cholinergic induction of dynamic hippocampal synaptic plasticity. Neuron 71, 155–165.

Gusev, A.G., Uteshev, V.V., 2010. Physiological concentrations of choline activate native alpha7-containing nicotinic acetylcholine receptors in the presence of PNU-120596 [1-(5-chloro-2,4-dimethoxyphenyl)-3-(5-methylisoxazol-3-yl)-urea]. J. Pharmacol. Exp. Ther. 332, 588–598.

Hille, B., 1992. Ionic Channels in Excitable Membranes. Sinauer Associates, Sunderland, MA.

Hurst, R., Rollema, H., Bertrand, D., 2012. Nicotinic acetylcholine receptors: from basic science to therapeutics. Pharmacol. Ther. (in press). Q3

Hurst, R.S., Hajos, M., Raggenbass, M., Wall, T.M., Higdon, N.R., Lawson, J.A., Rutherford-Root, K.L., Berkenpas, M.B., Hoffmann, W.E., Piotrowski, D.W., Groppi, V.E., Allaman, G., Ogier, R., Bertrand, S., Bertrand, D., Arneric, S.P., 2005. A novel positive allosteric modulator of the alpha7 neuronal nicotinic acetylcholine receptor: in vitro and in vivo characterization. J. Neurosci. 25, 4396–4405.

Jonas, P., 1995. Fast application of agonists to isolated membrane patches. In: Sakmann, B., Neher, E. (Eds.), Single Channel Recording. Plenum Press, New York and London, pp. 231–243.

Kalappa, B.I., Gusev, A.G., Uteshev, V.V., 2010. Activation of functional alpha7-containing nAChRs in hippocampal CA1 pyramidal neurons by physiological levels of choline in the presence of PNU-120596. PLoS One 5, e13964.

Khiroug, S.S., Harkness, P.C., Lamb, P.W., Sudweeks, S.N., Khiroug, L., Millar, N.S., Yakel, J.L., 2002. Rat nicotinic ACh receptor alpha7 and beta2 subunits co-assemble to form functional heteromeric nicotinic receptor channels. J. Physiol. 540, 425–434.

Komal, P., Evans, G., Nashmi, R., 2011. A rapid agonist application system for fast activation of ligand-gated ion channels. J. Neurosci. Methods 198, 246–254.

Lendvai, B., Kassai, F., Szajli, A., Nemethy, Z., 2012. alpha7 Nicotinic acetylcholine receptors and their role in cognition. Brain Res. Bull.. Q4

Lendvai, B., Vizi, E.S., 2008. Nonsynaptic chemical transmission through nicotinic acetylcholine receptors. Physiol. Rev. 88, 333–349.

Liu, Y., Dilger, J.P., 1991. Opening rate of acetylcholine receptor channels. Biophys. J. 60, 424–432.

Lozada, A.F., Wang, X., Gounko, N.V., Massey, K.A., Duan, J., Liu, Z., Berg, D.K., 2012. Glutamatergic synapse formation is promoted by alpha7-containing nicotinic acetylcholine receptors. J. Neurosci. 32, 7651–7661.

McCormack, T.J., Melis, C., Colon, J., Gay, E.A., Mike, A., Karoly, R., Lamb, P.W., Molteni, C., Yakel, J.L., 2010. Rapid desensitization of the rat 7 nAChR is facilitated by the presence of a proline residue in the outer beta-sheet. J. Physiol. 588, 4415–4429.

McKay, B.E., Placzek, A.N., Dani, J.A., 2007. Regulation of synaptic transmission and plasticity by neuronal nicotinic acetylcholine receptors. Biochem. Pharmacol. 74, 1120–1133.

Mike, A., Castro, N.G., Albuquerque, E.X., 2000. Choline and acetylcholine have similar kinetic properties of activation and desensitization on the alpha7 nicotinic receptors in rat hippocampal neurons. Brain Res. 882, 155–168.

Mike, A., Pesti, K., Szabo, A.K., Vizi, E.S., Mode of action of the positive modulator PNU-120596 on alpha7 nicotinic acetylcholine receptors. Neuropharmacology.

Papke, R.L., 2006. Estimation of both the potency and efficacy of alpha7 nAChR agonists from single-concentration responses. Life Sci. 78, 2812–2819.

Papke, R.L., 2010. Tricks of perspective: insights and limitations to the study of macroscopic currents for the analysis of nAChR activation and desensitization. J. Mol. Neurosci. 40, 77–86.

Papke, R.L., Meyer, E., Nutter, T., Uteshev, V.V., 2000. alpha7 receptor-selective agonists and modes of alpha7 receptor activation. Eur. J. Pharmacol. 393, 179–195.

Papke, R.L., Thinschmidt, J.S., 1998. The correction of alpha7 nicotinic acetylcholine receptor concentration-response relationships in Xenopus oocytes. Neurosci. Lett. 256, 163–166.

Paradiso, K.G., Steinbach, J.H., 2003. Nicotine is highly effective at producing desensitization of rat alpha4beta2 neuronal nicotinic receptors. J. Physiol. 553, 857–871.

Puchacz, E., Buisson, B., Bertrand, D., Lukas, R.J., 1994. Functional expression of nicotinic acetylcholine receptors containing rat alpha 7 subunits in human SH-SY5Y neuroblastoma cells. FEBS Lett. 354, 155–159.

Reitstetter, R., Lukas, R.J., Gruener, R., 1999. Dependence of nicotinic acetylcholine receptor recovery from desensitization on the duration of agonist exposure. J. Pharmacol. Exp. Ther. 289, 656–660.

Rozsa, B., Katona, G., Kaszas, A., Szipocs, R., Vizi, E.S., 2008. Dendritic nicotinic receptors modulate backpropagating action potentials and long-term plasticity of interneurons. Eur. J. Neurosci. 27, 364–377.

Sachs, F., 1999. Practical limits on the maximal speed of solution exchange for patch clamp experiments. Biophys. J. 77, 682–690.

Szasz, B.K., Mike, A., Karoly, R., Gerevich, Z., Illes, P., Vizi, E.S., Kiss, J.P., 2007. Direct inhibitory effect of fluoxetine on N-methyl-D-aspartate receptors in the central nervous system. Biol. Psychiatry 62, 1303–1309.

Uteshev, V.V., Meyer, E.M., Papke, R.L., 2002. Activation and inhibition of native neuronal alpha-bungarotoxin-sensitive nicotinic ACh receptors. Brain Res. 948, 33–46.

Valles, A.S., Roccamo, A.M., Barrantes, F.J., 2009. Ric-3 chaperone-mediated stable cell-surface expression of the neuronal alpha7 nicotinic acetylcholine receptor in mammalian cells. Acta Pharmacol. Sin. 30, 818–827.

Vizi, E.S., Lendvai, B., 1999. Modulatory role of presynaptic nicotinic receptors in synaptic and non-synaptic chemical communication in the central nervous system. Brain Res. Brain Res. Rev. 30, 219–235.

Williams, D.K., Peng, C., Kimbrell, M.R., Papke, R.L., 2012. Intrinsically low open probability of alpha7 nicotinic acetylcholine receptors can be overcome by positive allosteric modulation and serum factors leading to the generation of excitotoxic currents at physiological temperatures. Mol. Pharmacol. 82, 746–759.

Williams, D.K., Wang, J., Papke, R.L., 2011. Investigation of the molecular mechanism of the alpha7 nAChR positive allosteric modulator PNU-120596 provides evidence for two distinct desensitized states. Mol. Pharmacol..

Please cite this article in press as: Pesti, K., et al., Kinetic properties and open probability of α7 nicotinic acetylcholine receptors, Neuropharmacology (2014), http://dx.doi.org/10.1016/j.neuropharm.2014.01.034